

Testing quantum speedups in exciton transport through a photosynthetic complex using quantum stochastic walks

Pratyush Kumar Sahoo¹ and Colin Benjamin²

¹*Department of Physical Sciences, Indian Institute of Science Education & Research, Kolkata, India*

²*School of Physical Sciences, National Institute of Science Education & Research, HBNI, Jatni-752050, India**

Photosynthesis is a highly efficient process, nearly 100 percent of the red photons falling on the surface of leaves reach the reaction center and get transformed into energy. Quantum coherence has been speculated to play a significant role in this very efficient transport process which involves photons transforming to exciton's and then traveling to the reaction center. Studies on photosynthetic complexes focus mainly on the Fenna-Matthews-Olson complex obtained from green-sulfur bacteria. However, there has been a debate regarding whether quantum coherence results in any speedup of the exciton transport process. To address this we model exciton transport in FMO using a quantum stochastic walk(QSW) with either pure dephasing or with both dephasing and incoherence. We find that the QSW model with pure dephasing leads to a substantial quantum speedup as compared to a QSW model which includes both dephasing and incoherence.

I. INTRODUCTION

The first step of photosynthesis takes place via the antennae molecules called the chromophores. These antennae molecules loose electrons when light falls on them and an electron-hole pair or exciton is formed[1]. This exciton in turn has to reach the reaction center where the charge separation occurs and energy is stored. Usually these reaction centers are far in terms of molecular distance from the excited antennae molecule. But, this process of transferring the captured photon to the reaction centre is seen to exhibit an efficiency close to 100 percent. In 2007, it was reported[2] using "two dimensional Fourier transform electronic spectroscopy" (2D-FTES) that quantum coherence could be playing an important role in the exciton transport in Fenna-Matthews-Olson (FMO) complex found in green-sulphur bacteria. Later this was theoretically analyzed[3]. The exciton thus must not be following a classical random walk to get to the reaction center before its conversion to energy[1] rather the antennae molecules were operating via a search strategy called the quantum walk[3]. A quantum walker takes all possible paths, (like a superposed atom in the two-slit experiment) as opposed to classical random walker who must choose a single route. This gives quantum walk an advantage in the sense that it spreads with rate proportional to the time taken as compared to classical random walk which spreads as square root of time. Quantum coherence in FMO complex implies exciton transfer seen at life sustaining temperatures of 300K is aided by the quantum walk process which apparently takes place in presence of dephasing. Later in 2010, it was demonstrated[2] that quantum coherence was seen for nearly 300fs in FMO complex at 300K. Quantum coherence at normal ambient temperatures have also been detected in LHC2 complex found in bacteria[4], in spinach[5] and in a group of aquatic algae[6].

In Ref. [3] quantum walks were first used to study exciton transfer dynamics in FMO complex interacting with a thermal bath. Later, Hoyer, et. al., in Ref. [7] used a master equation approach with pure dephasing to model exciton transfer

in FMO. In Ref. [8] a more general form of quantum walk called the quantum stochastic walk(QSW) which is adaptable to include classical effects either only dephasing or both incoherence and dephasing was introduced. A QSW interpolates between classical random walk(CRW) and continuous-time quantum walk (CTQW) through a single parameter ω . ω is a measure of the amount of dephasing and/or incoherence built into the QSW. Later in Ref. [9] QSW was used to model FMO and results were compared with Ref. [7]. Our main aim in this paper is to test the prognosis that quantum effects do not lead to any speedup of the exciton transport from antenna to reaction center as was advanced in Ref. [7]. Quantum speedup of excitonic transport is measured via the localization time(t_{loc}). Localization time[7] is defined as time at which the onset of sub-diffusive transport occurs in the exciton transport process. The greater is the localization time, the more is the duration for which super-diffusive transport prevails. Thus, for significant speed up localization time must be large. In Ref. [7] localization time at both 77K and 300K is around 70fs. In our work, on the other hand, we find for the QSW model with pure dephasing localization time at 300K is more than that at 77K in accordance with the expectation of a quantum speedup. The main take home message of this work is that at life sustaining temperatures of 300K, the QSW model with pure dephasing leads to quantum speedup in exciton transport while in case of a QSW model with both dephasing and incoherence or the master equation approach of Hoyer, et. al., in Ref. [7] there is no quantum speedup seen at 300K.

The outline of the paper is as follows: in the next section we give details of the quantum stochastic walk used to model exciton transport in FMO and introduce the two models, one on incorporating pure dephasing in QSW and the other on including both incoherence and dephasing in the QSW. Subsequent to this we give details of the FMO complex, it's Hamiltonian and on how both QSW models are used to model exciton transport in FMO. In section III we plot the results of our simulations for total site coherence, site population, mean square displacement and localization time. In section IV we discuss our results and plots via two tables, the first for localization time and the second for other quantities. We end the paper and section IV with conclusion which includes a per-

* colin.nano@gmail.com

spective on future endeavors in this area.

II. QUANTUM STOCHASTIC WALK

Two variants of quantum walks are known- discrete-time quantum walk (DTQW)[10] and continuous time quantum walk (CTQW)[11]. A more general form of continuous time quantum walk called the quantum stochastic walk (QSW) was first introduced in Ref. [8]. It has the advantage of interpolating continuously from a classical random walk to a continuous time quantum walk and can address quantum walk processes which are coupled to an environment. QSW was derived from Kossakowski-Lindblad master equation[12, 13], which is used to describe quantum stochastic process and model open quantum systems. QSW is based on density matrix, dynamics of which is given by[8]-

$$\frac{d\rho(t)}{dt} = -(1-\omega)i[H, \rho(t)] + \omega \sum_{k=1}^K \left(\hat{L}_k \rho(t) \hat{L}_k^\dagger - \frac{1}{2} \left(\hat{L}_k^\dagger \hat{L}_k \rho(t) + \rho(t) \hat{L}_k^\dagger \hat{L}_k \right) \right) \quad (1)$$

where $\rho(t)$ is the density matrix representation of walker at time t . For QSW on any graph G , $\rho(t)$ is a $N \times N$ matrix with vertex states- $\{|1\rangle, \dots, |N\rangle\}$ as the basis, and elements $\rho_{ij}(t) = \langle i | \rho(t) | j \rangle$. $0 \leq \omega \leq 1$ is a parameter which interpolates between CRW and CTQW. For $\omega = 0$ both models of QSW considered, reduce to a CTQW. H is the Hamiltonian operator responsible for coherent dynamics. The index k has a unique value for each pair of i, j implying k has N^2 unique values, N being the number of vertices in the graph. The first term on the right hand side is responsible for coherent dynamics and the second term on right gives rise to incoherent dynamics via either only dephasing or both dephasing and incoherent scattering.

\hat{L}_k are Lindblad operators which are sparse $N \times N$ matrices. N being the total number of vertices of the underlying graph. For the purpose of modeling a QSW with only pure dephasing, the Lindblad operators are (see section 4.2 of Ref. [9] and Refs. [8, 14] for more details on modeling QSW with pure dephasing):

$$\hat{L}_k = \sqrt{|H_{ii}|} |i\rangle\langle i|. \quad (2)$$

wherein $H_{ii} = \langle i | H | i \rangle$ are the diagonal elements in the matrix representation of Hamiltonian operator H . In this model we have Lindblad operators corresponding to the diagonal entries of the density matrix. For $\omega = 1$ it can be shown[9] that:

$$\frac{d\rho_{ij}(t)}{dt} = \begin{cases} -\rho_{ij}(t), & i \neq j \\ 0, & i = j \end{cases} \quad (3)$$

Equation (3) shows that the off-diagonal terms of the density matrix which represent coherences die exponentially while the population(ρ_{ii}) remains constant. So, there is no transport at $\omega = 1$ limit for the pure dephasing model.

On the other hand, when modeling a QSW with both dephasing and incoherence, the Lindblad operators are chosen to be, (see also [8] and section 2 of Ref. [9])-

$$\hat{L}_k = \sqrt{|H_{ij}|} |i\rangle\langle j|, \quad (4)$$

with $H_{ij} = \langle i | H | j \rangle$ being the matrix elements of the Hamiltonian operator H . The Lindblad operators in Eq. 4 represent scattering between all pair of vertices. For $\omega = 1$, the QSW model with both dephasing and incoherence reduces to CRW[7].

III. MODELING EXCITON TRANSPORT IN FMO COMPLEX

In the photosynthetic process, energy gathered from light by antennae molecules is transmitted across the network of chlorophyll molecules to reaction centers [15]. This process is nearly 100% efficient as nearly all the red photons are captured and stored as energy. Experiments have revealed long-lasting quantum coherence in energy transport across a range of photosynthetic light-harvesting complexes[16–20]. One such light-harvesting complex is the Fenna-Matthews-Olson (FMO) complex from the green sulphur bacteria. The FMO complex consists of seven regions called chromophores, through which the exciton's propagate via hopping and it has been speculated that this propagation is aided by phase coherence[16].

A. Understanding exciton transport in FMO: the model of Hoyer, et. al.,[7]

To understand how quantum effects are important in the very efficient transfer of excitons at room temperatures, Hoyer, et. al. in Ref. [7] used a master equation approach to model exciton transport in FMO by incorporating dephasing into their model. The plot of total site coherence (Fig. 3(c) of [7]) for both 77K and 300K indicates the presence of coherence for nearly 500fs. Despite this long lived coherence, the plot of power law of mean square displacement(Fig. 3(b) of [7]) indicates that much of the transport occurs in the sub-diffusive regime. The super-diffusive nature of transport lasts for only 70fs, indicating localization time of 70fs at both temperatures of 77K and 300K. Hence, Hoyer, et. al., in Ref. [7] conclude that coherence in FMO does not yield dynamic speed up unlike that seen in quantum search algorithms, even though quantum coherence may last longer. The main conclusion of Ref. [7] was quantum coherent effects in a biological system like FMO lead to optimized or robust exciton transport, which is 100% efficient rather than any speedup of the transport. In this work we test this conclusion regarding speedup of the exciton transport via quantum stochastic walks(QSW). To this end, we employ two different approaches for incorporating incoherence into the QSW, the first pure dephasing (see Eq. (2)) and the second dephasing with incoherence (see Eq. (4)). Both the methods are explained in greater detail in the subsequent sections.

B. Modeling FMO using QSW

Earlier attempts [3, 7, 21] to model exciton transfer in FMO complex have used non-probability conserving master equations. These equations use loss terms to model absorption of exciton's by reaction centers and like QSW combine incoherent and coherent transport via a master equation approach. Here, we take another approach of adding an extra vertex and model FMO using probability conserving QSW. This was first done in Ref.[9]. This model is versatile and can reproduce pure dephasing transport as well as both dephasing and incoherent scattering, however, it does not have an explicit temperature dependence. Ref. [9] also made an incorrect comparison of the QSW model with both incoherence and dephasing to the model of Ref. [7] which includes only dephasing. In our work, we correct this and compare QSW with pure dephasing to the model of Ref. [7] to get a proper one to one correspondence between ω and temperature. Thus, we compare the plots of total site coherence versus time for various values of ω for QSW using pure dephasing with Fig. 3(c) of Ref.[7]. We find that $\omega = 0.19$ corresponds to a temperature of 77K and $\omega = 0.486$ corresponds to a temperature of 300K. Using $\omega = 0.19$ in the simulation of QSW with pure dephasing in FMO, the plot of site population versus time replicates Fig. 3(d) of [7] which is at 77K. First in sub-section 3.B.1 we model exciton transfer in FMO using pure dephasing, then in sub-section 3.B.2 both dephasing and incoherent scattering is considered. The QSW simulations shown in section IV use the *QSWalk* package[9, 22] for *Wolfram Mathematica*.

1. Modeling exciton transport in FMO via QSW with pure dephasing

FMO has 7 chromophore sites (see Fig.1). The excitation starts at initial site 6 and gets absorbed at site 3[23], the reaction center. QSW is a probability conserving process, in contrast Hoyer, et. al.'s model[7] doesn't conserve probability. To have a one-to-one correspondence between both of our QSW models with the model of Hoyer, et. al., we include a sink to model absorption. Therefore, in our QSW simulations, an extra site numbered 8 is added, which acts as a sink, see Ref. [9]. This extra vertex is added using a directed edge and does not take part in the coherent transport via the Hamiltonian. The time evolution of the density matrix for our QSW is given by:

$$\begin{aligned} \frac{d\rho}{dt} = & -(1 - \omega)i[H, \rho(t)] \\ & + \omega \sum_{k=1}^K (\hat{L}_k \rho(t) \hat{L}_k^\dagger - \frac{1}{2}(\hat{L}_k^\dagger \hat{L}_k \rho(t) + \rho(t) \hat{L}_k^\dagger \hat{L}_k)) \quad (5) \end{aligned}$$

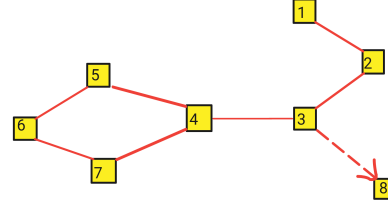


Figure 1. Simplified figure of FMO complex. The chromophores are numbered from 1 to 7. Vertex 8 is the sink. Exciton travels from site 6 and finds it's way to site 3 the reaction center. The lines between the chromophore sites represent dipolar coupling between them. In fact, there is coupling between every site which is represented by the Hamiltonian given in Eq. (6)[23]. But only the couplings above $15cm^{-1}$ have been shown in Fig. 1, similar to Ref. [7]. One can assume the exciton to be following the path according to Fig. 1 with sufficient confidence.

We use the Hamiltonian obtained by Adolphs and Renger[23]:

$$H = \begin{bmatrix} 200 & -96 & 5 & -4.4 & 4.7 & -12.6 & -6.2 \\ -96 & 320 & 33.1 & 6.8 & 4.5 & 7.4 & -0.3 \\ 5 & 33.1 & 0 & -51.1 & 0.8 & -8.4 & 7.6 \\ -4.4 & 6.8 & -51.1 & 110 & -76.6 & -14.2 & -67 \\ 4.7 & 4.5 & 0.8 & -76.6 & 270 & 78.3 & -0.1 \\ -12.6 & 7.4 & -8.4 & -14.2 & 78.3 & 420 & 38.3 \\ -6.2 & -0.3 & 7.6 & -67 & -0.1 & 38.3 & 230 \end{bmatrix} \quad (6)$$

The units of energy are cm^{-1} (we follow the usual spectroscopy convention of expressing energy in terms of the wavelength of photon with that energy, i.e., $1cm^{-1} \equiv 1.23984 \times 10^{-4}eV$). The model uses the above Hamiltonian, padded with zeros to construct an 8×8 matrix, so as to describe coherent evolution. For QSW using pure dephasing we use the Lindblad operators- defined as in Eq. 2 $\hat{L}_k = \sqrt{|H_{ii}|} |i\rangle \langle i|$. There is an unique value of k for each vertex pair i, j . The sum in Eq. (5) extends over all i, j such that $k = N^2$. An extra Lindblad operator is used for the sink: $\hat{L}_k = \sqrt{\alpha} |8\rangle \langle 3|$, where α determines the rate of absorption at the sink (here $\alpha = 100$ as in Ref.[9]). Through these Lindblad operators we incorporate incoherent scattering as well as dephasing. The initial density matrix is given as $\rho(0) = |6\rangle \langle 6|$, assuming the initial excitation being localized at site 6. Since temperature doesn't appear in QSW we try to make a one to one correspondence between our simulation of the total site coherence(see section IV.A below) with the same simulation in Ref. [7]. This gives us the equivalent ω values for particular temperatures. $\omega = 0.19$ corresponds to temperature of 77K and $\omega = 0.486$ corresponds to 300K. This equivalence between ω and temperature is got by comparing the plot of total site coherence Fig. 2(a) of this work, with Fig. 3(c) of Ref. [7]. The procedure to calculate the total site coherence is given in the next section.

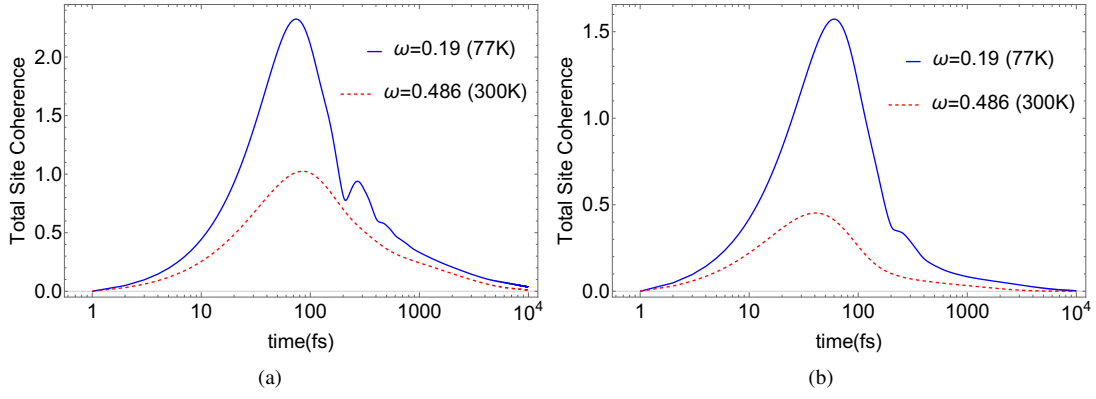


Figure 2. Total site coherence versus time using (a) Pure dephasing (b) Dephasing and incoherent scattering. Comparing Fig. 2(a) with Fig. 3(c) of Ref. [7], we get the equivalent values for ω at temperatures of 77K and 300K.

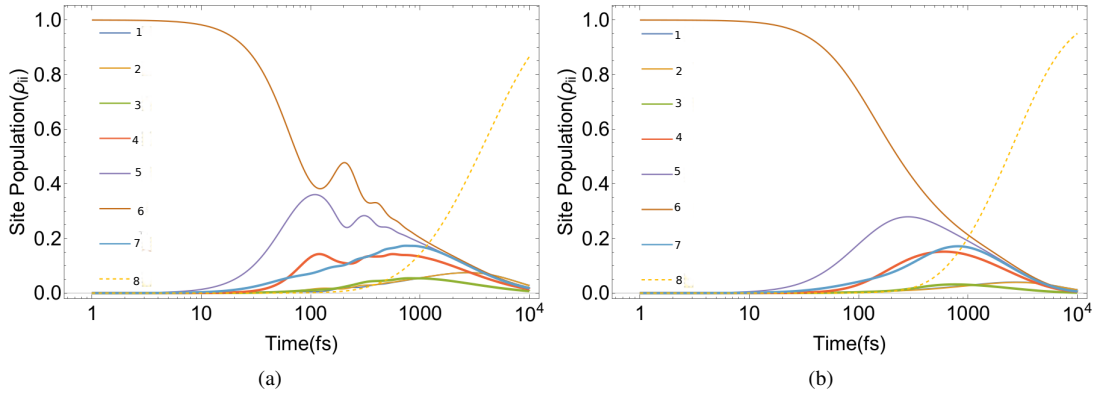


Figure 3. Site population (ρ_{ii}) versus time for pure dephasing at temperatures (a) 77K ($\omega = 0.19$) (b) 300K ($\omega = 0.486$). Fig. 3(a) is in excellent agreement with Fig. 3(d) of Ref.[7].

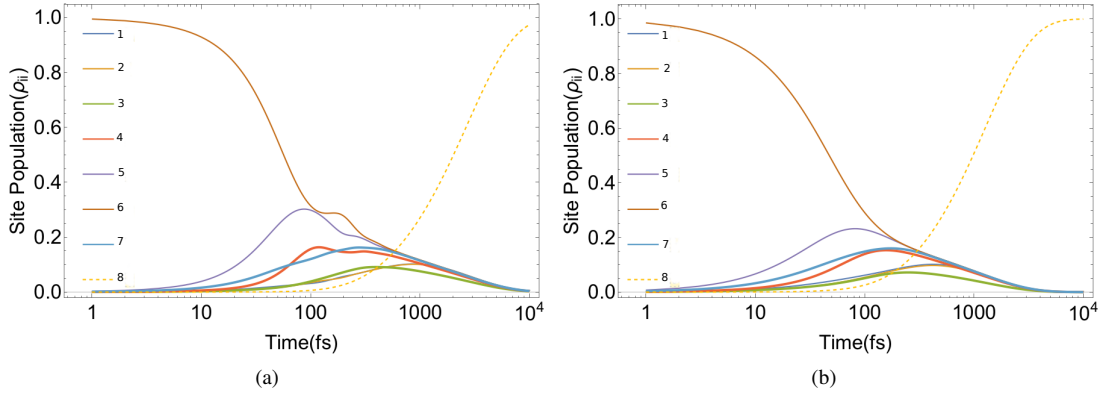


Figure 4. Site population (ρ_{ii}) versus time for dephasing and incoherence at temperatures (a) 77K ($\omega = 0.19$) (b) 300K ($\omega = 0.486$).

2. Modeling exciton transport in FMO via QSW with both dephasing and incoherent scattering

For the case of QSW model with both dephasing and incoherence[8] we use the set of Lindblad operators, see Eq. 4, $\hat{L}_k = \sqrt{|H_{ij}|}|i\rangle\langle j|$. It is important to note that for this model

of QSW as defined in [8] we get CRW ($\omega = 1$) and CTQW ($\omega = 0$) as two extreme cases. For the sink we use the same Lindblad operator as previous: $\hat{L}_k = \sqrt{\alpha}|8\rangle\langle 3|$, with $\alpha = 100$ determining the absorption rate at the sink. We now make a detailed study of exciton transport in FMO complex focusing on total site coherence, site population, mean square displace-

ment and localization time better understand the exciton dynamics of a FMO complex and compare with the results of Ref. [7] especially with regards to the localization time.

IV. RESULTS

A. Total Site Coherence

Total site coherence is defined as sum of the absolute value of each off-diagonal element of the density matrix in the site basis. Finite valued off-diagonal elements of a density matrix indicate coherence. Total site coherence is a measure of the coherence present in the FMO complex. The QSW does not have explicit temperature dependence. It has a single parameter ω and to get an explicit temperature dependence for our QSW model via ω we compare plots of total site coherence versus time (for pure dephasing) at different values of ω with Fig. 3(c) of Ref. [7] and find that $\omega = 0.19$ corresponds to a temperature of 77K while $\omega = 0.486$ corresponds to 300K (see Fig. 2(a) which depicts total site coherence for exciton transport in QSW with pure dephasing). Ref. [7] uses master equation with pure dephasing to model exciton transfer in FMO. Hence the plot of total site coherence using QSW with pure dephasing has been compared with the respective plot (Fig.3(c)) of Ref. [7] to obtain the correspondence between ω and temperature.

B. Site Population

Site population of the i^{th} site in the FMO complex is defined as ρ_{ii}^{th} element of the density matrix ρ . Site population of the i^{th} site represents the probability of finding the exciton at that site. Initially the exciton is at site 6. Using Eq. 2 and the Mathematica code(QSWalk[9, 22]), we calculate the time evolution of the population of each site via QSW. Site population versus time for QSW with pure dephasing at both 77K (i.e., $\omega = 0.19$) and 300K (i.e., $\omega = 0.486$) has been plotted in Fig. 3. Fig. 3(a) is in excellent qualitative agreement with Fig. 3(d) of Ref. [7]. We see that with increase in temperature the oscillations die down faster with time. Site population versus time for QSW with both incoherence and dephasing is given in Fig. 4. Further, with incoherent scattering incorporated the oscillations in site population die out too(see Figures 4(a) and 4(b)).

C. Mean Square Displacement

Mean square displacement is defined as[7]

$$\langle x^2 \rangle = \frac{Tr(\rho x^2)}{Tr(\rho)}, \quad (7)$$

where, x is the displacement from the initial site and ρ being the density matrix. The mean square displacement depicts how fast the exciton moves away from the initial site.

The mean square displacement versus time has been plotted in Fig. 5 for both pure dephasing and dephasing with incoherence. By assuming that mean square displacement follows a power law, see Ref. [7] for reasons behind this assumption, we have

$$\langle x^2 \rangle = t^b, \text{ and taking logarithm on both sides,} \\ \text{we get- } \log \langle x^2 \rangle = b \log t. \quad (8)$$

where t denotes time. Exponent 'b' versus time has been plotted in Fig. 6, which has been obtained by plotting slope of log-log plot of mean square displacement (slope of Fig. 5). For $b > 1$ the transport is called super diffusive and $b < 1$ corresponds to sub-diffusive transport. These definitions are with respect to classical random walk (CRW) which follows diffusive transport at $b = 1$. In Fig. 3(b) of Ref.[7] the plots of power law versus time shows the transition from super diffusive to sub-diffusive transport at 70fs for both 77K as well as 300K. In the plots of power law versus time for QSW with pure dephasing (Fig. 6(a)) and QSW with both dephasing and incoherence (Fig. 6(b)) shows that the time for this transition time is different at different temperatures (corresponding to different ω). More about this result has been explained in the next section on localization time. Further, the *Mathematica* code and method of calculation for mean square displacement, power law b and localization time(t_{loc}) has been provided in Appendix A.

D. Localization time

The localization time(t_{loc}) is defined[7] as the time at which the transition of power law b occurs from super diffusive to the sub-diffusive regime, i.e., the power b goes below 1. t_{loc} values have been given in Table I. We see that for the QSW model with pure dephasing there is indeed a speed up at 300K as t_{loc} increases at 300K ($\omega = 0.486$) as compared to 77K ($\omega = 0.19$). Even if we change the initial state of the exciton to be at site 1 instead of site 6, we get speed up at 300K for the QSW model with pure dephasing, the t_{loc} values being 63fs at 77K and 98fs at 300K. This result is the key takeaway message of our work. However, in case of QSW model with both dephasing and incoherence there is on the other hand a slow down instead of speed up, t_{loc} reduces from 54fs at 77K to 15fs at 300K. These results are in stark contrast to that seen by Hoyer, et. al.'s work[7] where t_{loc} doesn't change from 77K to 300K. An explanation for these findings on localization time has been provided in Appendix B and Appendix C by comparing site population. One can clearly see in Fig. 8 (Appendix B), that the exciton population at each site invariably reaches a peak at 300K later than that at 77K. Thus, time for ρ_{ii} to peak at 77K is always less than the time for ρ_{ii} to peak at 300K for QSW model with pure dephasing. One can also see in Fig. 8(red dots), the plot of Hoyer, et. al., for each site and one can see that it is always earlier to peak than for QSW model with pure dephasing at 77K.

In contrast in Fig. 9 (Appendix C), one can clearly see that the exciton population at each site invariably reaches a peak earlier at 300K than at 77K. Thus, time for ρ_{ii} to reach a peak

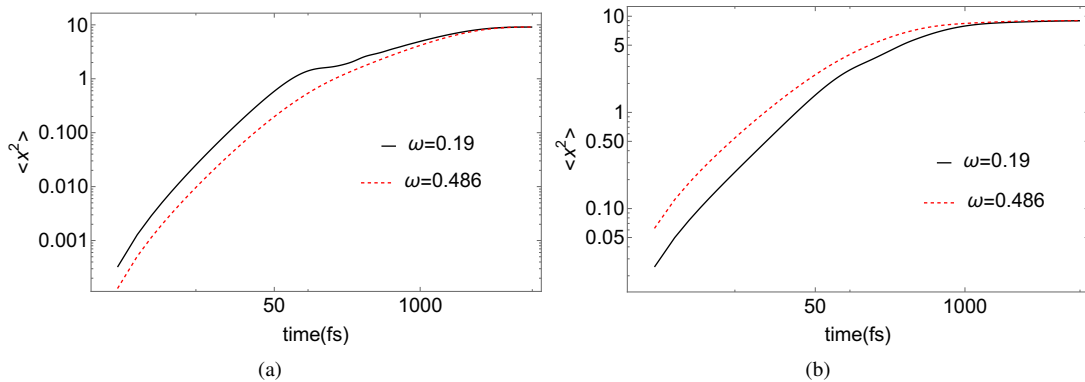


Figure 5. Log-log plot of mean square displacement versus time for (a) pure dephasing (b) dephasing and incoherence.

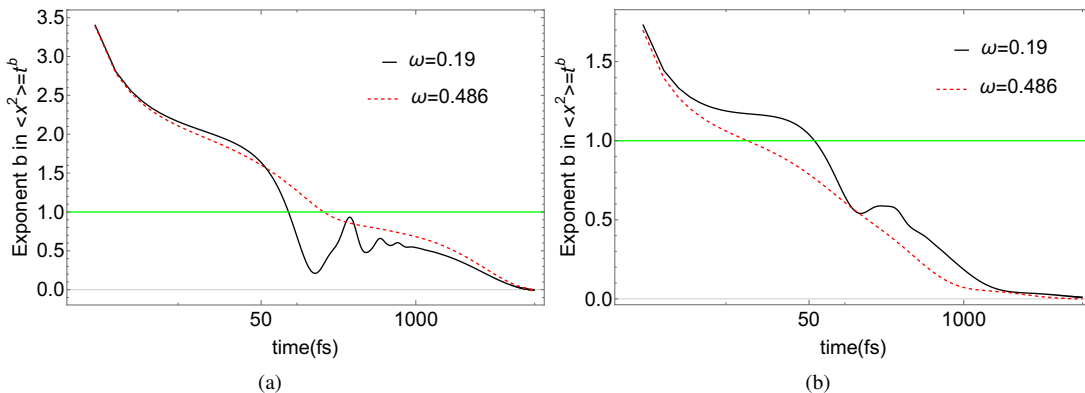


Figure 6. Power law b versus time for (a) pure dephasing (b) dephasing and incoherence.

Table I. Localization time comparison for Model of Hoyer, et. al., Ref. [7], QSW with pure dephasing (Eq. 2) and QSW with dephasing and incoherence (Eq. 4) in exciton transfer through FMO.

	Model of Hoyer, et. al., Ref. [7]	QSW with pure dephasing (Eq. 2)	QSW with dephasing and incoherence (Eq. 4)
t_{loc} at 77K (in femto-secs)	70	81	54
t_{loc} at 300K (in femto-secs)	70	150	15

at 77K is always greater than time for ρ_{ii} to reach a peak at 300K for QSW model with both dephasing and incoherence.

V. DISCUSSION AND CONCLUSION

Table I compares the localization time for the three models. It is evident that the localization time for pure dephasing model increases at 300K as compared to 77K. This is in line with the quantum Goldilocks effect [1, 24] which predicted increase in speed of exciton transport at a temperature nearly equal to the room temperature. The model of Ref. [7] nor the QSW model with both dephasing and incoherence can explain this effect as the localization time is same for both 77K and 300K in case of Ref. [7] while in case of the QSW model with both dephasing and incoherence there is a slow down instead of speed up, rendering any quantum effect meaningless. This result has major implication for studies in exciton

transport through FMO. It means a QSW model with pure dephasing is best able to explain not only the robust transport of exciton but also the quantum advantage which delivers the necessary speed up to exciton transport process. Hence, the model using QSW with pure dephasing best represents the exciton transport in FMO. This is line with earlier study which predicted [24] maximum efficiency of exciton transport process in FMO around room temperatures than very low temperatures like 77K.

To check that our model of exciton transfer using QSW is in line with earlier studies, we check the transport process at very high coherence which corresponds to near absolute zero temperature. It has been shown in Ref. [24] that an optimum amount of coherence is required for maximum efficiency of any quantum transport process. This has been called the quantum Goldilocks effect. If the environment is too cold, i.e. $\omega \rightarrow 0$ or fully coherent exciton transport, the exciton will wander aimlessly without getting anywhere. In this case the

Table II. Comparison of three models (Model of Hoyer, et. al.,[7], QSW with pure dephasing and QSW with both incoherence and dephasing) for exciton transfer in FMO.

	Model of Hoyer <i>et. al.</i> , [7]	QSW model with pure dephasing	QSW model with incoherence and dephasing
Total Site Coherence	Same as in case of QSW with pure dephasing.(Fig.3(c) in [7])	Decreases with rise in temperature or ω (Fig.2(a))	Decreases with rise in temperature or ω (Fig.2(b))
Site Population	Similar to QSW using pure dephasing.(Fig.3(d) in [7])	Oscillations are more prominent for dephasing but decrease with rise in temperature(Fig.3)	Oscillations in site population vanish with increasing temperature(Fig.4)
Power law b	Super diffusive to sub-diffusive transition occurs at $70fs$ for both $77K$ and $300K$. (Fig.3(b) in [7])	Super-diffusive to sub-diffusive transition occurs at $81fs$ for $77K$ and $150fs$ for $300K$ (Fig.6(a))	Super-diffusive to sub-diffusive transition occurs at $54fs$ for $77K$ and $15fs$ for $300K$ (Fig.6(b))

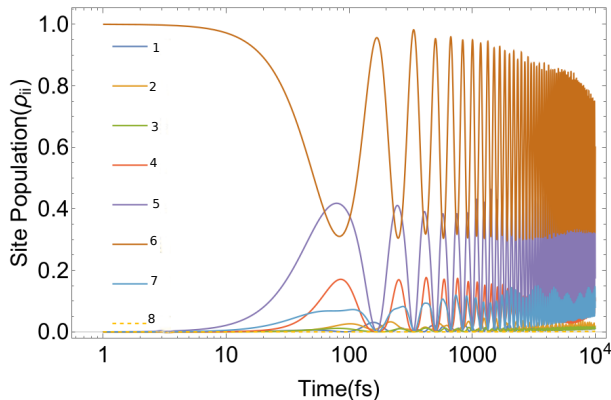


Figure 7. Plot of site population versus time for $\omega = 0.001$ showing persisting oscillations and the exciton coming back to initial site i.e. site 6 repeatedly for QSW model with pure dephasing.

exciton will behave like a wave but will not be able to propagate due to destructive interference. We have shown this effect by putting $\omega = 0.001$ (highly coherent) and looking at the site population. The plot of site population (see Fig.7) shows that the exciton keeps coming back to initial site, that is site 6. Even after 10^4 femto-seconds the exciton can be found with a very high probability at site 6. This shows there is essentially no transport at very low temperatures when transport is fully coherent. In Table II we compare the three models of exciton transfer in FMO complex as regards the other quantities like total site coherence, site population and exponent in the power law. Having seen that the QSW model with pure dephasing is the closest to describing exciton transport with quantum effects, we see that the total site coherence behaves very similarly in the other models too. Oscillations in site population in both QSW model with pure dephasing and in Hoyer, et. al.'s model mirror each other while for QSW model with both dephasing and incoherence there is a marked difference with oscillations almost disappearing. Finally, exponent b in the power law again matches the localization time results seen in Table I.

To conclude, quantum stochastic walk is a powerful tool to model exciton transport in FMO complex. QSW has a single parameter ω that controls the amount of decoherence present in the model. With increase in ω transport becomes more in-

coherent. The temperature dependence enters the model via ω . This seems intuitive, as with increase in thermal fluctuations the amount of coherence should decrease. Therefore, we compare the plots of total site coherence versus time for different values of ω for QSW with pure dephasing with Fig. 3(c) of Ref.[7] to get the corresponding values of ω . Then we model FMO with QSW with both dephasing as well as incoherent scattering. We find that the model QSW model with pure dephasing has increased localization time at $300K$ as compared to $77K$ in line with the quantum Goldilocks effect. The QSW model with both dephasing and incoherence nor the model of Ref. [7] was able to explain this effect as the localization time is same for both $77K$ and $300K$. QSW model with pure dephasing gives speed up at $300K$ as compared to $77K$, while QSW with both dephasing and incoherent scattering gives slow down at $300K$. Future works can include studying the transport efficiency in FMO using different initial states, like superposed states, e.g., $\frac{1}{\sqrt{2}}(|1\rangle + |6\rangle)$ as was done in Ref. [25]). It will also be interesting to study the exciton transfer dynamics via QSW when say entangled initial states, see Ref. [26], are present.

VI. ACKNOWLEDGEMENTS

PKS would like to thank the National Institute of Science Education and Research, HBNI, Jatni 752050, India for providing hospitality and Dept. of Science and Technology (DST) for the INSPIRE fellowship. CB would like to thank Science and Engineering Research Board (SERB) for funding under MATRICS grant "Nash equilibrium versus Pareto optimality in N-Player games" (MTR/2018/000070).

VII. APPENDIX

A. Mathematica codes for power law b and localization time

The *Mathematica* code for plotting mean square displacement and power law b is given here. This has been used to generate Fig. 5(a) and Fig. 6(a), which is for the case of QSW model with pure dephasing. For the case of QSW model with both dephasing and incoherence, we use the Hamiltonian H (defined in the code) instead of H' and generate the Lindblad

set. This code makes use of *QSWalk*[9, 22] package. For the mean square displacement, we first need to have some notion of distance for the sites of FMO. We refer to Fig. 1 of the FMO complex. The lines between the chromophore sites represent dipolar coupling between them. In fact, there is coupling between every site which is represented by the Hamiltonian given in Eq. 6[23]. But only the couplings above 15cm^{-1} have been shown in Fig. 1[7]. Since the magnitude of coupling less than 15cm^{-1} is pretty low, as also was done in Ref. [7], we choose to ignore these couplings, i.e., these sites are effectively decoupled for the purpose of calculating the effective paths from initial site to reaction center, implying the exciton to be following the path according to Fig. 1. We can then assign a position to each site accordingly. This approach has also been done in Ref. [7] (Fig. 1(b) of [7]). Since the initial excitation is at site 6, it is defined to be the origin of FMO. Then according to Fig. 1, we define the sites 5 and 7 to be at a distance of 1 unit away from site 6. Similarly, site 4 to be 2 units, 3 being 3 units, 2 being 4 units and 1 to

be 5 units of distance away from 6. Since site 8 is the sink which was added for probability conservation, we assign site 8 to be 3 units away from site 6. With this information we define the operator x as shown in the code. This operator is an 8×8 matrix which has eigenvectors as the sites represented as column vectors and eigenvalues being their respective distance from site 6, as defined above. We know that expectation value of any operator \hat{A} is given by $\frac{\text{Tr}(\rho\hat{A})}{\text{Tr}(\rho)}$, ρ being the density operator. So the mean square displacement is given by:

$$\langle x^2 \rangle = \frac{\text{Tr}(\rho x^2)}{\text{Tr}(\rho)} \quad (9)$$

We have implemented the above equation in the code to find mean square displacement. The slope of the log-log plot of mean square displacement will give the power law b , as explained in the section called mean square displacement. The intersection of the power law b plot with $y = 1$ line will give us the localization time.

```

<< QSWalk
energyUnit =2 Pi Quantity["ReducedPlanckConstant"]
Quantity["SpeedOfLight"]/Quantity["Centimeters"]
actionUnit = Quantity["ReducedPlanckConstant"]
timeUnit = UnitConvert[actionUnit/energyUnit, "Femtoseconds"]
N[timeUnit]
H0 = ( {
  {200, -96, 5, -4.4, 4.7, -12.6, -6.2},
  {-96, 320, 33.1, 6.8, 4.5, 7.4, -0.3},
  {5, 33.1, 0, -51.1, 0.8, -8.4, 7.6},
  {-4.4, 6.8, -51.1, 110, -76.6, -14.2, -67},
  {4.7, 4.5, 0.8, -76.6, 270, 78.3, -0.1},
  {-12.6, 7.4, -8.4, -14.2, 78.3, 420, 38.3},
  {-6.2, -0.3, 7.6, -67, -0.1, 38.3, 230}
} );
x = SparseArray[{{1, 1} -> 5, {2, 2} -> 4, {3, 3} -> 3, {4, 4} -> 2, {5, 5} -> 1,
{6, 6} -> 0, {7, 7} -> 1, {8, 8} -> 3}, {8, 8}];
H = SparseArray[ArrayRules[H0], {8, 8}];
H' = SparseArray[{{1, 1} -> 200, {2, 2} -> 320, {3, 3} -> 0, {4, 4} -> 110, {5, 5} -> 270,
{6, 6} -> 420, {7, 7} -> 230}, {8, 8}];
rho0 = SparseArray[{{6, 6} -> 1}, {8, 8}];
LkSet = Append[LindbladSet[H'], SparseArray[{{8, 3} -> 10.}, {8, 8}]];
dt = Quantity["Femtoseconds"]/timeUnit //N
omega = 0.19;
Clear[rho];
qsw[rho_] = QuantumStochasticWalk[H, LkSet, omega, rho, dt]
n = 10000; tfs = Range[0, n];
pt = Chop@NestList[qsw, rho0, n];
a = List[];
slope = List[];
k = 1;
While[k < 10000,
p = pt[[k]];
x2 = x.x; m = x2.p;
value = Tr[m]/Tr[p];
a = Append[a, value]; k++;
p1 = ListLogLogPlot[a, Joined -> True, PlotStyle -> Black, PlotRange -> All,
Frame -> True, FrameLabel -> {"time(fs)", Exponent b, RotateLabel -> True};
s = 1;
While[s < 9999,
s1 = (Log[a[[s + 1]]] - Log[a[[s]]))/(Log[s + 1] - Log[s]);
slope = Append[slope, s1]; s++;
p11 = ListLogLinearPlot[slope, PlotRange -> All, Joined -> True, PlotStyle -> Black,
PlotLegends -> {"\[Omega]=0.19"}, Frame -> True, FrameLabel -> {"time(fs)", "Power_law_b", RotateLabel -> True};

omega = 0.486;
Clear[rho]; qsw[rho_] = QuantumStochasticWalk[H, LkSet, omega, rho, dt]
n = 10000;
tfs = Range[0, n];
pt = Chop@NestList[qsw, rho0, n];
a = List[];
slope = List[];

```

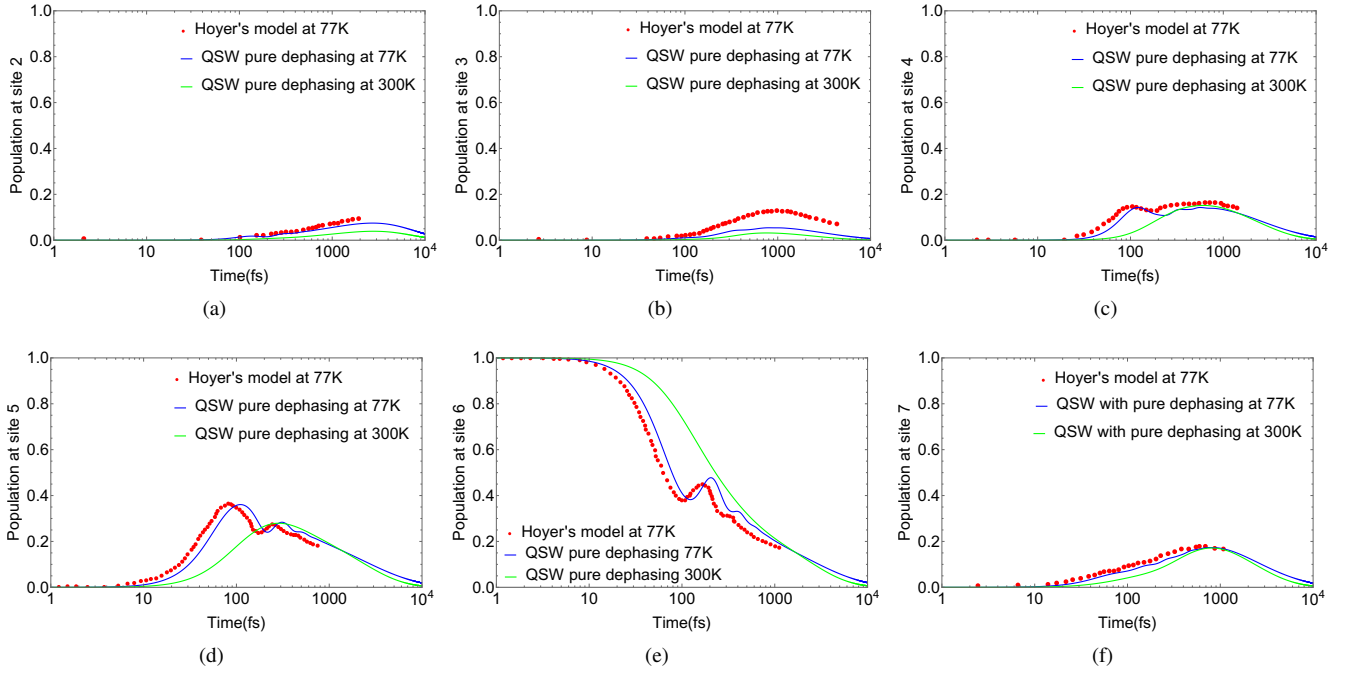


Figure 8. Site population versus time for various sites at 77K. Hoyer's model has been compared with QSW with pure dephasing model.

```

k = 1;
While[k < 10000,
  p = pt[[k]];
  x2 = x.x;
  m = x2.p;
  value = Tr[m]/Tr[p];
  a = Append[a, value]; k++]
s = 1;
While[s < 9999,
  s1 = (Log[a[[s + 1]]] - Log[a[[s]]))/(Log[s + 1] - Log[s]);
  slope = Append[slope, s1]; s++]
p1 = ListLogLinearPlot[slope, PlotRange -> All, Joined -> True,
  PlotStyle -> {Red, Dashed}, PlotLegends -> {"\[\Omega]=0.486"},
  AxesLabel -> {"Time(fs)", "Power_law_b"}];

p2 = ListLogLogPlot[a, Joined -> True, PlotStyle -> {Red, Dashed},
  PlotRange -> All, PlotRange -> All, Frame -> True,
  FrameLabel -> {"time(fs)",
  "Mean_square_displacement"}, RotateLabel -> True];
Show[p1, p2]
p13 = Plot[1, {x, 0, 1000}, PlotStyle -> Green, Frame -> True,
  FrameLabel -> {"time(fs)", "power_law_b"}, RotateLabel -> True]
Show[p11, p12, p13]

```

B. Comparison of QSW model with pure dephasing and Hoyer's model at 77K

We have plotted in Fig. 8 the evolution of the exciton population at different sites for QSW model with pure dephasing at $\omega = 0.19$ (temperature= 77K) and the same for Hoyer, et. al.'s model at 77K, we also put the plots for QSW model with pure dephasing at 300K for comparison. As Hoyer, et. al.'s model did not have the plot for site 1, we omit site 1 from this analysis. To show the plot for Hoyer, et. al.'s model at 77K, we have extracted data from Fig. 3(d) of Ref. [7] using GRABIT[27] tool for MATLAB. We see that there is remarkable similarity in the plot at 77K for QSW with pure dephasing and Hoyer's model. But, these plots do not coincide, which leads to slightly different localization time. From Figures 8(a-f) we see that the site population for each site in the pure dephasing model at $\omega = 0.19$ (temperature= 77K) reaches a peak at a slightly later time as compared to Hoyer's model at 77K. This agrees with the slightly higher localization time of 81fs in case of QSW with pure dephasing as compared to 70fs in the case Hoyer's model. Also from Figures 8(a-f) we see that for QSW model with pure dephasing at $\omega = 0.486$ (temperature= 300K) the population at each site reaches a peak even later. This again agrees with the increased localization time, which is 150fs for QSW model with pure dephasing at 300K. In conclusion, localization time is

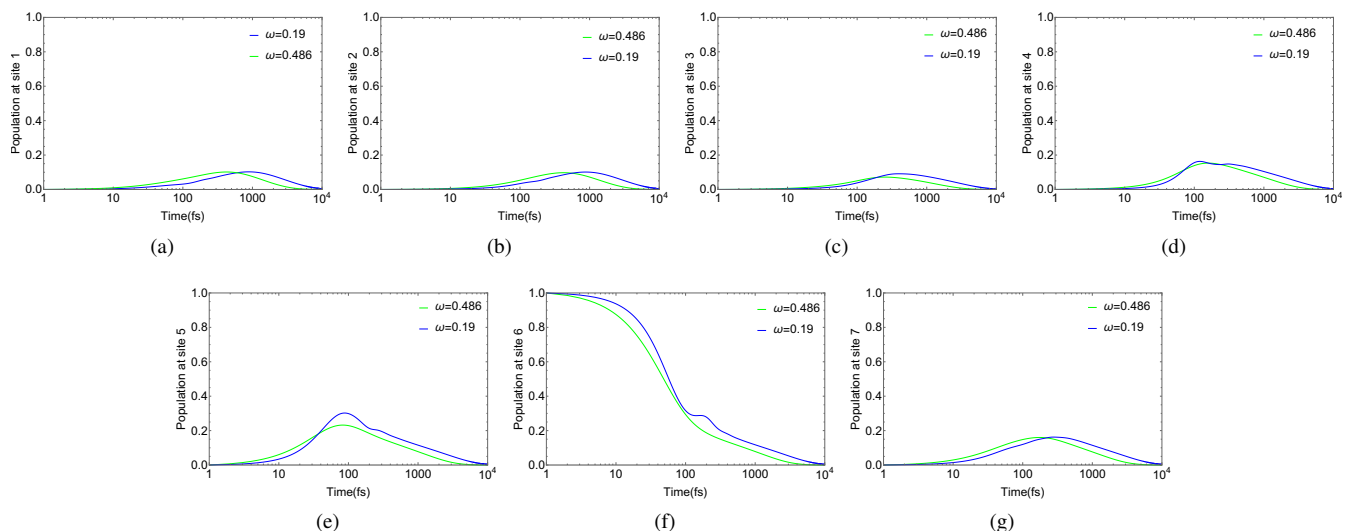


Figure 9. Site population versus time for various sites at 77K and 300K for QSW model with both dephasing and incoherent scattering.

more at 300K than at 77K for QSW model with pure dephasing. This explains the major departure from Hoyer’s model which has same localization time, that is $70fs$ for both 77K and 300K. A housekeeping note on the use of GRABIT[27] tool, that in Fig. 3(d) of Ref. [7] the x-axis is in logarithmic scale. GRABIT can only be used for uniformly scaled axes. So we set the lower limit of the x-axis as 0 and upper limit as 4. So that after converting to log scale the limits will be 1 and 10^4 , as in the original graph. We extract the data points by manually clicking on the graph. We then scale the extracted x-axis data to log scale with base 10 to get the exact data points, see also Ref. [28] wherein GRABIT has also been employed for log axis similarly.

C. Site population plots for QSW with incoherent scattering and dephasing

Here, we have plotted (Fig. 9) the evolution of exciton population at each site in the QSW model with both dephasing and incoherence at $\omega = 0.19$ (temperature= 77K) and $\omega = 0.486$ (temperature= 300K). We note from each of the plots Fig. 9(a-g) that at 300K the exciton population reaches the peak at a much faster rate than at 77K. This leads to decrease in the localization time for 300K implying a slow down. Thus, rendering the QSW model with both dephasing and incoherence ineffective in explaining the possible quantum speed up expected in exciton transport in FMO complex.

-
- [1] J. Al-Khalili and J. McFadden, *Life on the Edge: The Coming of Age of Quantum Biology* (Penguin Random House, UK, 2014).
- [2] G. Panitchayangkoon, D. Hayes, K. A. Fransted, J. R. Caram, E. Harel, J. Wen, R. E. Blankenship, and G. S. Engel, Long-lived quantum coherence in photosynthetic complexes at physiological temperature, **107**, 12766 (2010).
- [3] M. Mohseni, P. Rebentrost, S. Lloyd, and A. Aspuru-Guzik, Environment-assisted quantum walks in photosynthetic energy transfer, *The Journal of Chemical Physics* **129**, 174106 (2008).
- [4] I. P. Mercer, Y. C. El-Taha, N. Kajumba, J. P. Marangos, J. W. G. Tisch, M. Gabrielsen, R. J. Cogdell, E. Springate, and E. Turcu, Instantaneous mapping of coherently coupled electronic transitions and energy transfers in a photosynthetic complex using angle-resolved coherent optical wave-mixing, *Phys. Rev. Lett.* **102**, 057402 (2009).
- [5] T. R. Calhoun, N. S. Ginsberg, G. S. Schlau-Cohen, Y.-C. Cheng, M. Ballottari, R. Bassi, and G. R. Fleming, Quantum coherence enabled determination of the energy landscape in light-harvesting complex ii, *The Journal of Physical Chemistry B* **113**, 16291 (2009).
- [6] E. Collini, C. Y. Wong, K. E. Wilk, P. M. G. Curmi, P. Brumer, and G. D. Scholes, Coherently wired light-harvesting in photosynthetic marine algae at ambient temperature, *Nature* **463**, 644 (2010).
- [7] S. Hoyer, M. Sarovar, and K. B. Whaley, Limits of quantum speedup in photosynthetic light harvesting, *New Journal of Physics* **12**, 065041 (2010).
- [8] J. D. Whitfield, C. A. Rodríguez-Rosario, and A. Aspuru-Guzik, Quantum stochastic walks: A generalization of classical random walks and quantum walks, *Phys. Rev. A* **81**, 022323 (2010).
- [9] P. E. Falloon, J. Rodriguez, and J. B. Wang, Qswalk: A mathematica package for quantum stochastic walks on arbitrary graphs, *Computer Physics Communications* **217**, 162 (2017).

- [10] Y. Aharonov, L. Davidovich, and N. Zagury, Quantum random walks, *Phys. Rev. A* **48**, 1687 (1993).
- [11] E. Farhi and S. Gutmann, Quantum computation and decision trees, *Phys. Rev. A* **58**, 915 (1998).
- [12] A. Kossakowski, On quantum statistical mechanics of non-hamiltonian systems, *Reports on Mathematical Physics* **3**, 247 (1972).
- [13] G. Lindblad, On the generators of quantum dynamical semi-groups, *Communications in Mathematical Physics* **48**, 119 (1976).
- [14] V. Kendon, Decoherence in quantum walks- a review, *Mathematical Structures in Computer Science* **17**, 1169 (2007).
- [15] Y.-C. Cheng and G. R. Fleming, Dynamics of light harvesting in photosynthesis, *Annual Review of Physical Chemistry* **60**, 241 (2009).
- [16] G. S. Engel, T. R. Calhoun, E. L. Read, T.-K. Ahn, T. Manical, Y.-C. Cheng, R. E. Blankenship, and G. R. Fleming, Evidence for wavelike energy transfer through quantum coherence in photosynthetic systems, *Nature* **446**, 782 (2007).
- [17] H. Lee, Y.-C. Cheng, and G. R. Fleming, Coherence dynamics in photosynthesis: Protein protection of excitonic coherence, *Science* **316**, 1462 (2007).
- [18] A. Ishizaki and G. R. Fleming, Theoretical examination of quantum coherence in a photosynthetic system at physiological temperature, *Proceedings of the National Academy of Sciences* **106**, 17255 (2009).
- [19] T. R. Calhoun, N. S. Ginsberg, G. S. Schlau-Cohen, Y.-C. Cheng, M. Ballottari, R. Bassi, and G. R. Fleming, Quantum coherence enabled determination of the energy landscape in light-harvesting complex ii, *The Journal of Physical Chemistry B* **113**, 16291 (2009).
- [20] E. Collini, C. Y. Wong, K. E. Wilk, P. M. G. Curmi, P. Brumer, and G. D. Scholes, Coherently wired light-harvesting in photosynthetic marine algae at ambient temperature, *Nature* **463**, 644 (2010).
- [21] M. B. Plenio and S. F. Huelga, Dephasing-assisted transport: quantum networks and biomolecules, *New Journal of Physics* **10**, 113019 (2008).
- [22] J. B. W. Peter E. Falloon, Jeremy Rodriguez, *QSWalk Download*, <https://data.mendeley.com/datasets/8rwd3j9zhk/1>.
- [23] J. Adolphs and T. Renger, How proteins trigger excitation energy transfer in the fmo complex of green sulfur bacteria, *Biophysical Journal* **91**, 2778 (2006).
- [24] S. Lloyd, M. Mohseni, A. Shabani, and H. Rabitz, The quantum goldilocks effect: on the convergence of timescales in quantum transport (2011).
- [25] J. Zhu, S. Kais, P. Rebentrost, and A. Aspuru-Guzik, Modified scaled hierarchical equation of motion approach for the study of quantum coherence in photosynthetic complexes, *The Journal of Physical Chemistry B* **115**, 1531 (2011).
- [26] A. Ishizaki and G. R. Fleming, Quantum superpositions in photosynthetic light harvesting: delocalization and entanglement, *New Journal of Physics* **12**, 055004 (2010).
- [27] *jiro* (2020). *GRABIT*, <https://www.mathworks.com/matlabcentral/fileexchange/7173-grabit>, MATLAB Central File Exchange. Retrieved April 2, 2020.
- [28] W. Weijtjens, *How do we use the GRABIT tool to extract data from a semi logarithmic plot in MATLAB?*, https://www.researchgate.net/post/How_do_we_use_the_GRABIT_tool_to_extract_data_from_a_semi_logarithmic_plot_in_MATLAB.